European Review for Medical and Pharmacological Sciences 2019; 23: 5382-5391

RUNX3 protects against acute lung injury by inhibiting the JAK2/STAT3 pathway in rats with severe acute pancreatitis

S. LI[1,2], H.-Z. CUI[3], C.-M. XU[1,4], Z.-W. SUN[5], Z.-K. TANG[6], H.-L. CHEN[1]

[1]Department of General Surgery, The First Affiliated Hospital of Dalian Medical University, Dalian, Liaoning Province, China
[2]Department of Traditional Chinese Medicine, Affiliated Municipal Central Hospital of Dalian Medical University, Dalian, Liaoning Province, China
[3]Department of General Surgery, Affiliated Zhongshan Hospital of Dalian University, Dalian, Liaoning Province, China
[4]Department of Traditional Chinese Medicine, Obstetrics and Gynecology Hospital of Dalian Medical University, Dalian, Liaoning Province, China
[5]Department of Emergency Medicine, Affiliated Zhongshan Hospital of Dalian University, Dalian, Liaoning Province, China
[6]Department of Emergency Medicine, The First Hospital of Lanzhou University, Lanzhou, Gansu Province, China

Abstract. – OBJECTIVE: Acute lung injury (ALI) is the most common complication of severe acute pancreatitis (SAP) in the early stage, which causes systemic inflammatory response and organ damage. Human runt-associated transcription factor 3 gene (RUNX3) has been reported to participate in various inflammatory diseases. However, the exact role of RUNX3 in SAP and its-related ALI remains unclear.

MATERIALS AND METHODS: To establish the model of SAP, rats were retrogradely injected with 5% sodium taurocholate (1 mg/kg body weight) into the biliary-pancreatic duct. Cytokine level in serum was measured by ELISA, and the polymorphonuclear neutrophil (PMN) was isolated from rat's blood 12 h-post SAP induction.

RESULTS: We found RUNX3 expression was significantly decreased with the progression of SAP. Both pancreas damages and cytokine production abilities were reduced in RUXN3-overexpressed SAP rats compared with control rats. Moreover, SAP-associated ALI was also improved upon RUNX3 overexpression in SAP rats. RUNX3 upregulation enhanced PMN apoptosis and inhibited Janus kinase 2/signal transducer and activator of transcription 3 (JAK2/STAT3) phosphorylation.

CONCLUSIONS: Our study indicates that RUNX3 protects against SAP and SAP-associated ALI through controlling PMN apoptosis and regulating JAK2/STAT3 signaling pathway. RUNX3 could be regarded as a potent therapeutic target in SAP for future studies.

Key Words.
Severe acute pancreatitis, Acute lung injury, RUNX3, Inflammation, JAK2/STAT3 signaling.

Introduction

Acute pancreatitis (AP) is defined as a local inflammation in the pancreas, which is occurred by erratic activation of zymogen within the pancreas. Dysregulation of zymogen leads to autodigestion, inflammation, edema, vascular damage, and ultimately gives rise to cell death[1-3]. As a subtype of AP, severe acute pancreatitis (SAP) can cause several complications and more than 25% mortality[4,5]. In SAP, hyperproduction and secretion of inflammatory cytokines such as interleukin (IL)-1β, IL-6 and tumor necrosis factor (TNF)-α, would lead to pancreatic tissue necrosis, therefore affecting peripheral organs[6]. Acute lung injury (ALI) is a common complication of SAP in the early stage of the disease, which is the main cause of death in SAP patients[7]. SAP patients with ALI usually exhibited hypoxemia and dyspnea, accompanied by diffuse alveolar damage and polymorphonuclear neutrophils (PMN) infiltration in the lung. PMN play a critical role in pathogenesis of SAP-associated ALI by altering its lifespan and migrating to the site of inflammation[8]. PMN apoptosis is reported to be the key to suppression of inflammation during SAP. Extension of the PMN lifespan seriously affects SAP recovery and further result in the secondary tissue damages[8].

Janus kinase/signal transducer and activator of transcription (JAK/STAT) signaling are involved in various physiological and pathological processes, including immune responses, cellular homeostasis, cell proliferation, and malignant trans-

Corresponding Author: Hailong Chen, MD; e-mail: HailongChen159@163.com

formation[9,10]. As one of 7 members of the STAT family, STAT3 participates in cellular responses to cytokines and growth factors as transcription factors[11,12]. STAT3 is activated via JAK2-dependent phosphorylation and JAK2-independent phosphorylation[13]. Previous studies have demonstrated JAK2/STAT3 signaling could be activated by various cytokines including TNF-α, IL-1β and IL-6, which participate in the progression of inflammatory response[14,15]. Although multiple animal studies reported JAK2/STAT3 signaling was elevated in pancreatic acinar cells of AP rats[16,17], however, the effects of JAK2/STAT3 signaling on SAP-associated ALI remained largely unknown.

Human runt-associated transcription factor 3 (RUNX3) is a member of the runt domain family, which plays an important role in process of inflammation[18,19]. For instance, RUNX3 regulates transforming growth factor (TGF)-β-mediated functions of dendritic cell, and its loss results in airway inflammation[20]. Impairment of RUNX3 in white blood cells is associated with spontaneous colitis and gastric mucosal hyperplasia[21], while the exact role of RUNX3 in SAP and its-related ALI remains unclear. Recently, TNF receptor-associated factor 6 (TRAF6), direct targeting of RUNX3, has been identified as a protective factor in the progression of lipopolysaccharide (LPS)-induced AP[22,23]. Therefore, we speculated that RUNX3 could also regulates SAP and SAP-associated ALI. In this study, protective effects of RUNX3 on SAP and SAP-associated ALI were investigated, and the underlying regulatory mechanism was explored. Our findings improve our understanding of molecular machinery of SAP pathogenesis and hopefully provides insights into future development of therapeutic strategies targeting SAP and SAP-associated ALI.

Material and Methods

Reagents

Sodium taurocholate and Histopaque 1119/1077 Gradients were purchased from Sigma-Aldrich (St. Louis, MO, USA). Chloral hydrate was purchased from Tianjin Kemiou Chemical Reagent Co (Tianjin, China). Xylene, ammonium chloride (NH_4Cl), formalin and ethanol were purchased from Wako Pure Chemical Industries Ltd (Osaka, Japan).

Animal Experiments

Adult male Sprague Dawley (SD) rats (220-250 g) were purchased from Experimental Animal Center at Dalian Medical University (Dalian, China). Animal experiments were approved by the Animal Care and Use Committee of Dalian Medical University (Dalian, China) and were performed according to National Institutes of Health Guidelines for the Care and Use of Laboratory Animals[24]. Rats were housed at room temperature (22-26°C) with a 12 h light/12 h dark cycle. Food and water were provided ad libitum. Body weight of each rat was recorded every week. Totally, 36 SD rats of specific pathogen free (SPF) grade were selected as each group, named (1) Sham, (2) SAP and (3) SAP + RUNX3.

To induce SAP, rats were anesthetized with 10% chloral hydrate (3.5 mL/kg body weight) and the surgical field was exposed. The proximal bile duct was temporarily occluded at the hepatic portal by a vascular clamp, followed by retrograde injection of 5% sodium taurocholate (1 mg/kg body weight) in the distal end of the biliary-pancreatic duct. Changes of biliary-pancreatic duct and pancreatic tissues including congestion, edema, and hemorrhage were observed for 5 min. Subsequently, the vascular clamp was removed and the incision was sutured. Sham rats were anesthetized in the same manner without sodium taurocholate injection.

For RUNX3 overexpression experiment, rats were intravenous injected (i.v.) with Ad-RUNX3 ($1*10^9$) and Ad-control into the tail of rats 7 days pre-sodium taurocholate injection, when pulsatile blood appeared in the needle hub, Ad-RUNX3 was injected with a continuous and slow movement. Adenoviral vector containing RUNX3 was purchased by Shanghai GenePharma Co., Ltd. (Shanghai, China). All procedures were approved by the First Affiliated Hospital of Dalian Medical University Ethics Review Committee for Animal Experimentation (Experiment number 20170114XA) and were performed to minimize the number of animals used and their suffering.

Hematoxylin & Eosin (H&E) Staining

Three rats were randomly selected and sacrificed. Their tissues were fixed with 10% formalin solution for 24 h, followed by dehydration using ethanol. After transparent using xylene, tissues were embedded in Tissue-Tek OCT compound (Sakura Finetek, Torrance, CA, USA) and cooled at 4°C. Five micrometers tissue sections of pancreases and lung were baked in an oven at 60°C overnight, and xylene was dewaxed for 15 min. Tissue sections were stained by H&E Stain Kit (Maraval LifeSciences, Burlingame, CA, USA). The fume hood was air-dried and neutral resin

was sealed. Histopathological analysis was determined by double-blind scoring in terms of edema, hemorrhage, necrosis, and inflammatory cell infiltration according to Schmidt criteria.

Quantitative Real-Time Polymerase Chain Reaction (qRT-PCR)

Total RNAs were extracted from rat tissues using TRIzol Reagent (Invitrogen, Carlsbad, CA, USA). After RNase-free DNase (TaKaRa Biotechnology, Dalian, China) treatment, RNAs were reverse-transcribed to cDNA using a SuperScript IV First-Strand Synthesis System (Invitrogen, Carlsbad, CA, USA) following the instructions provided by the manufacturer. The PCR amplification conditions consisted a total of 45 cycles of pre-denaturation for 60 sec at 95°C, followed by denaturation 30 sec at 94°C, annealing at 60°C for 60 sec, and extension for 60 sec at 72°C. Expression level of RUNX3 was measured by SYBR-green master mix (Thermo Fisher Scientific, Waltham, MA, USA) using ViiA™7 Real-Time PCR System (Thermo Fisher Scientific). PCR program was set up as follows: an initial denaturing at 95°C for 10 sec, 40 cycles 95°C for 5 sec, and 60°C for 30 sec, followed by a melting curve analysis. Expression of β-*actin* was used as internal control.

Primer sequences (5'→3') used in this study were designed as follow:

- *Runx3*, forward: GCAACGCTTCCGCTGTCA, reverse: GGCTTTGGTCTGGTCCTCTATC.
- β-*actin*, forward, CGTGCGTGACATTAAAGAG, reverse, TTGCCGATAGTGATGACCT.

Lung Wet/Dry Weight Ratio

To measure the total amount of lung water, rats were dissected under anesthesia, and their lung weight was measured immediately after its excision. Lung tissues were then dried for 72 h at 50°C. Wet/dry weight ratio was calculated.

Bronchoalveolar Lavage Fluid (BALF)

Rats were anesthetized and euthanized by exsanguination. Their tracheas were surgically exposed and intubated with a syringe catheter. Lung tissues were lavage with 1 ml pre-warmed PBS and repeated 5 times. Five milliliters of BALF was collected from each rat and cells in BALF were pelleted by centrifugation at 500 g for 10 min at 4°C. Cells were then suspended in cold 1xPBS and counted by FACs.

Detection of Amylase Activity

To test the activity of amylase in serum, serum was collected from each group as indicated time and analyzed by Amylase Assay Kit (Abcam; Cambridge, MA, USA) according to the manufacturer's instructions. Briefly, serum was mixed with substrate ethylidene-pNP-G7 to produce smaller fragments that are eventually modified by α-glucosidase, causing the release of a chromophore. After incubation for 1 h in the dark, the absorbance was measured at 405 nm by a microplate reader (Bio-Rad, Hercules, CA, USA).

Measurement of Cytokines

Pro-inflammatory cytokines including IL-1β, IL-6, and TNF-α were measured using ELISA kit (R&D systems; Minneapolis MN, USA) according to manufacturer's instructions. In brief, the serum was incubated for 2 h at room temperature in 96-well plates coated with anti-IL-1β, anti-IL-6, and anti-TNF-α antibodies, respectively. After washing, the capture antibody was added and incubated for 2 h at room temperature. The reaction was measured by modulation of the absorbance at 405 nm.

Western Blotting

Protein from the tissue homogenates or PMN lysate were washed by 1xPBS, and then protein concentrations were measured using a BCA Protein Assay Kit (Thermo Fisher Scientific). 15 μg proteins were subjected to SDS-PAGE electrophoresis, separated and transferred onto polyvinylidene difluoride (PVDF) membrane (Immobilon-P; EMD Millipore, Darmstadt, Germany). The membrane was blocked with 5% of skill milk in TBS-T for 1 h and then incubated with primary antibody against RUNX3 (#9647, Cell Signaling, Danvers, MA, USA), Fas (ab82419, Abcam), FasL (ab231011, Abcam), Bax (#2772, Cell Signaling), cleaved caspase-3 (#9661, Cell Signaling), Bcl-xL (#2762, Cell Signaling), phosph-JAK2 (#3776, Cell Signaling), JAK2 (#3230, Cell Signaling), phosph-STAT3 (#9134, Cell Signaling), STAT3 (#4904, Cell Signaling) and GAPDH (#5174, Cell Signaling) overnight at 4°C. After washing three times with TBS-T, the membrane was incubated with appropriate secondary antibodies at room temperature for 1 h. As an internal control, GAPDH was measured by using an anti-GAPDH antibody (ab9486, Abcam) and an HRP-conjugated anti-rabbit antibody (GE Healthcare Life Science, Tokyo, Japan). Protein bands were detected using Luminata Forte Western HRP Substrate (Millipore, Billerica, MA, USA) with a Bio-Rad ChemiDox XRS+ imaging system (Bio-Rad, Hercules, CA, USA).

PMN Isolation

2.5 ml of Histopaque 1077 mg/ml was layered onto 2.5 ml of Histopaque 1119. Five milliliters of blood were placed on the top of the gradient mixture, thus forming a three-level gradient including Histopaque 1119, Histopaque 1077 and blood. Tube was centrifuged for 30 min in a swinging rotor centrifuge at 400 g. The superior part containing the ring of mononuclear cells was discarded. A second ring was the ring of target, which was collected and transferred to another tube to be washed with NH_4Cl 0.83% (w/v) to eliminate the erythrocytes. Finally, cells were washed with 1xPBS and 1xHBSS (pH=7.2) at 270 g for 10 min, followed by resuspension of cells using 1 ml HBSS containing 0.1% gelatin.

PMN Apoptosis Analysis

12 h post-SAP induction, PMN were isolated and washed with phosphate buffered saline, followed by cell resuspension. The supernatant was discarded by centrifugation at 1000 rpm at 4°C for 10 min. Then, cells were resuspended in 150 µl of 10 mM HEPES (pH=7.4), 140 mM NaCl and 2.5 mM $CaCl_2$, and placed on ice for 5 min. A further 50 µl of buffer containing 5 µl propidium iodide (PI) and 10 µl Annexin V-FITC were added. Cells were incubated at room temperature in the dark for 15 min after mix. A flow cytometric analysis FACs Calibur (BD Biosciences, San Jose, CA, USA) and FlowJo software (Tree Star, Ashland, OR, USA) were used to analyze cell apoptosis and calculate the apoptosis rate.

Statistical Analysis

Data were presented as means ± S.D. To determine statistical significance, GraphPad Prism 7 (GraphPad Software, SanDiego, CA, USA) was used to perform one-way ANOVA followed by Tukey's post hoc *t*-test for multiple comparisons or Student's *t*-tests when comparing 2 conditions. Probabilities <0.05 were considered statistically significant in this study (*p<0.05, **p<0.01, ***p<0.001).

Results

RUNX3 Overexpression Attenuates SAP in Rats

In SAP rats, we found RUNX3 transcription was reduced by SAP in a time-dependent manner compared with sham rats (Figure 1A). Consequently, protein level of RUNX3 in serum was also decreased upon SAP (Figure 1B), indicating RUNX3 was associated with SAP.

We noted tissue damages including interstitial edema, massive neutrophil infiltration, and focal necrosis were clearly observed in the pancreas of rats (Figure 2B), and the activity of amylase increased along with the induction time of SAP (Figure 2C). Simultaneously, histological analysis of lung section showed that pulmonary interstitial was highly congested, most of the alveolar spaces are significantly widened, and alveolar cavity is partially fused into partial atrophy of the pulmonary vesicle (Figure 2D). Large numbers of neu-

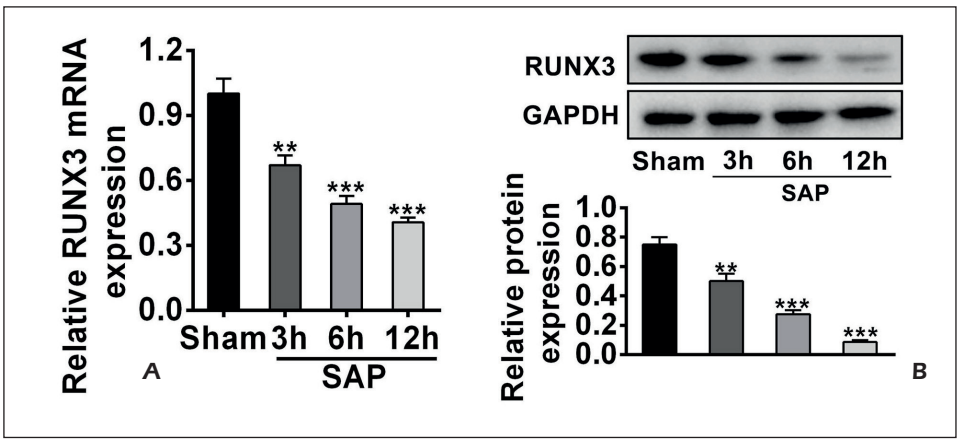

Figure 1. Expression of RUNX3 in SAP rat models. The serum was collected from each group of rats. Level of RUNX3 in the serum was measured by qRT-PCR for transcripts (**A**) and by Western blotting for protein (**B**). (Mean±S.D; n=10; **p<0.01, ***p<0.001).

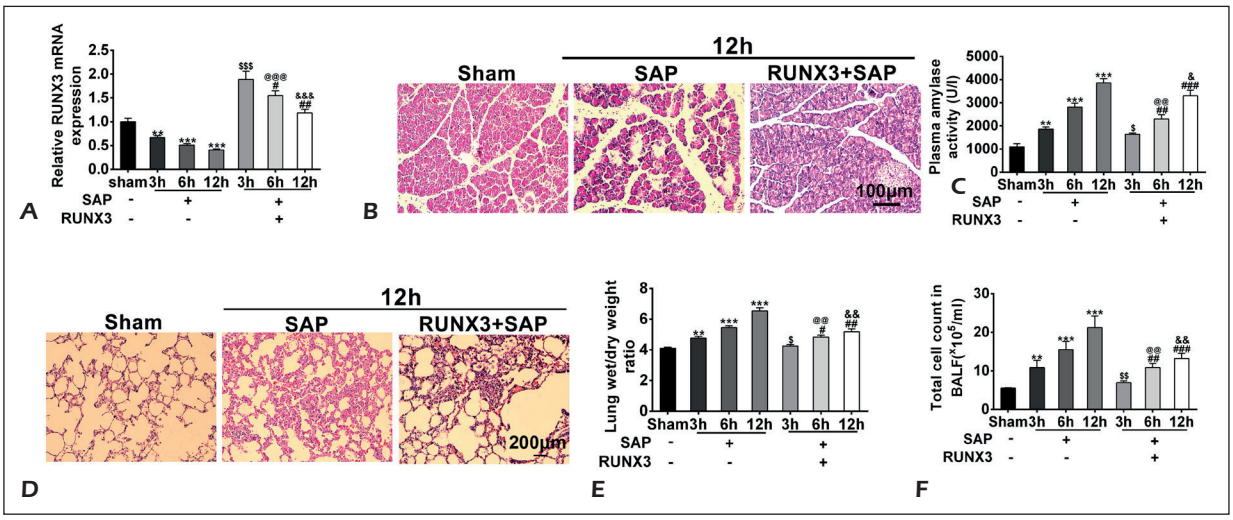

Figure 2. Tissue damage in SAP upon RUNX3 overexpression. mRNA level of RUNX3 in rat serum was quantified by qRT-PCR (**A**). The histopathology analysis of pancreas (**B**) and lung (**D**) was performed by H&E staining. Amylase activity in serum was measured by ELISA (**C**). Wet/dry weight ratio was determined to assess lung water content (**E**), and the total cell number in BALF was analyzed by FACs (**F**). (Mean±S.D; n=3; *vs.* control, $^{**}p<0.01$, $^{***}p<0.001$; $^{\#}p<0.05$, $^{\#\#}p<0.01$, $^{\#\#\#}p<0.001$; RUNX3 + SAP 3 h *vs.* SAP 3 h, $^{\$}p<0.05$, $^{\$\$}p<0.01$, $^{\$\$\$}p<0.001$; RUNX3 + SAP 6 h *vs.* SAP 6 h, $^{@@}p<0.01$, $^{@@@}p<0.001$; RUNX3 + SAP 12 h *vs.* SAP 12 h, $^{\&}p<0.05$, $^{\&\&}p<0.01$, $^{\&\&\&}p<0.001$).

trophil infiltrations in the pulmonary interstitial and the formation of visible microthrombus were also present in the lung of SAP rats (Figure 2D). As shown in Figure 2E-F, SAP also resulted in an elevated lung wet/dry weight ratio and total cell numbers of BALF. This evidence strongly demonstrated an SAP rat model was generated, and ALI was induced by SAP in these rats.

To further investigate the exact effects of RUNX3 on SAP, we injected SAP rats using Ad-RUNX3 intravenously (Figure 2A). Interestingly, the SAP-induced pancreas damages and the activity of amylase were significantly reduced by RUNX3 overexpression compared with that in SAP rats (Figure 2B-C). Moreover, RUNX3 upregulation decreased lung damages, lung wet/dry weight ratio as well as cell numbers in BALF (Figure 2D-2F). Therefore, these results suggested RUNX3 was critically involved in SAP as a negative regulator.

Anti-Inflammatory Effect of RUNX3 on SAP

We then evaluated whether RUNX3 was involved in the SAP-associated inflammation. Levels of a series index of inflammation, including of IL-1β, IL-6 and TNF-α, increased in serum (Figure 3A), pancreas (Figure 3B) as well as lung (Figure 3C) after SAP induction in a time-dependent manner. RUNX3 overexpression markedly reduced pro-inflammatory cytokines in pancreas, serum, and lung, respectively (Figure 3A-3C), indicating RUNX3 could indeed inhibit inflammation under SAP condition. RUNX3 acted as an anti-inflammatory factor against SAP.

RUNX3 Regulates PMN Apoptosis Upon SAP Condition

Given PMN was reported to play a critical role in the development of inflammation[8], we sought to clarify the regulation mechanism of inflammation regarding effects of RUNX3 on PMN apoptosis. We discovered 25% of PMN was PI^+ Annexin V^+ cells in Sham rat, and percentage of these PI and Annexin V double positive cells was decreased in SAP rats (Figure 4A). It is intriguing that RUNX3 upregulation in SAP rats significantly enhanced PI^+ Annexin V^+ PMN (Figure 4A), indicating RUNX3 positively regulated PMN apoptosis. In parallel study was performed by analysis of classical apoptosis signaling pathway via Western blotting. As shown in Figure 4B, RUNX3 overexpression in SAP rats upregulated Fas/FasL and Bax expression compared with SAP rats. Correspondingly, Bcl-xL, a negative regulator of Bax, was inhibited under RUNX3 overexpression. Reversely, Caspase-3, a downstream signal of these proteins, was activated (Figure 4B). These results supported our hypothesis that PMN played an anti-inflammatory role against SAP, suggesting RUNX3 contributed PMN-mediated inflammation resistance.

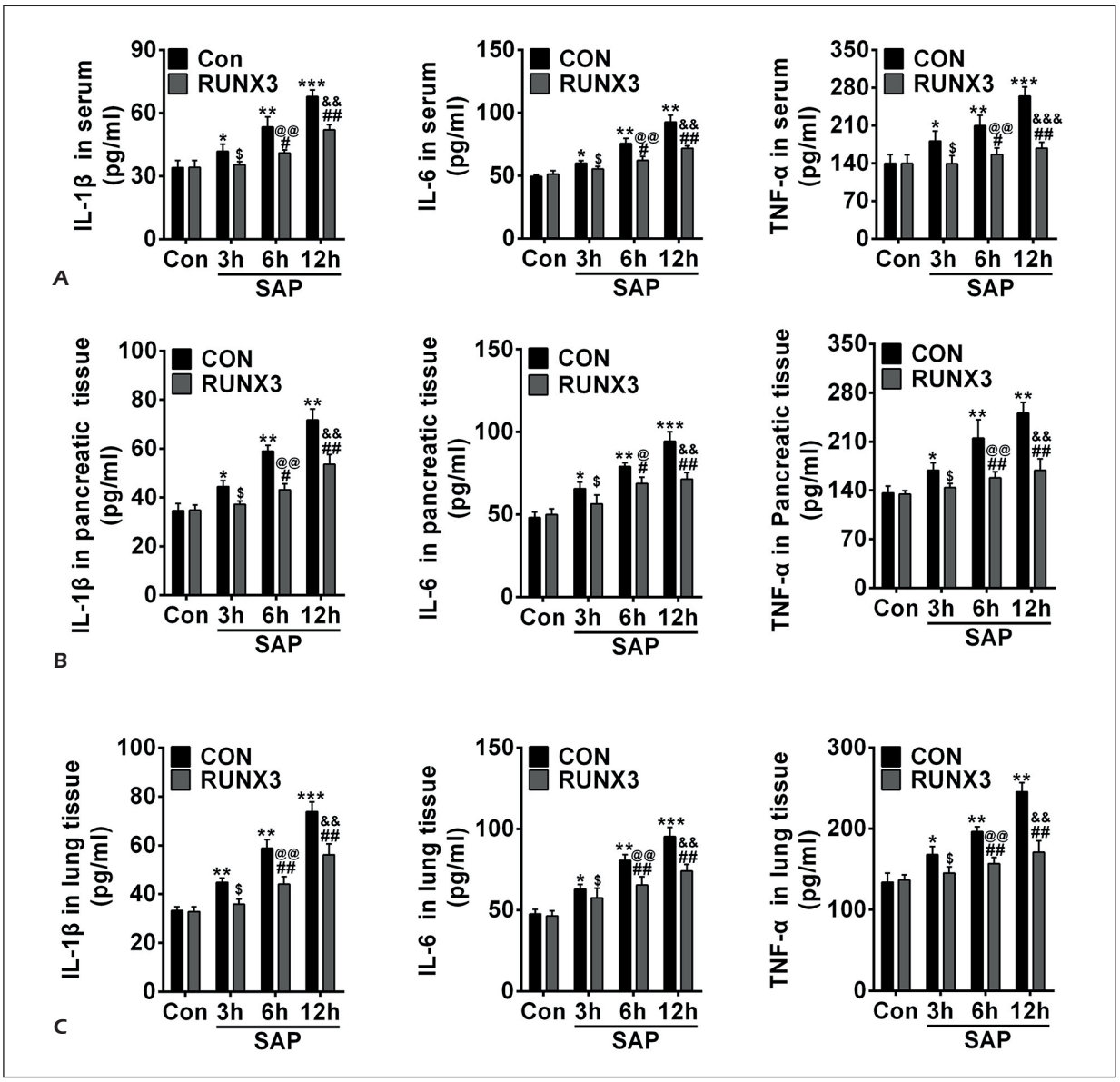

Figure 3. RUNX3 overexpression inhibits cytokine production in SAP model of rat. Cytokine IL-1β, IL-6 and TNF-α levels in serum (**A**), in pancreatic (**B**) and in lung (**C**) were measured by ELISA, respectively. (Mean±S.D; n =3; *vs.* control, *$p<0.05$, **$p<0.01$, ***$p<0.001$; RUNX3 overexpression *vs.* control, $^{\#}p<0.05$, $^{\#\#}p<0.01$, $^{\#\#\#}p<0.001$; RUNX3 + SAP 3 h *vs.* SAP 3 h, $^{\$}p<0.05$; RUNX3 + SAP 6 h *vs.* SAP 6 h, $^{@}p<0.05$, $^{@@}p<0.01$; RUNX3 + SAP 12 h *vs.* SAP 12 h, $^{\&\&}p<0.01$, $^{\&\&\&}p<0.001$).

Protective Effect of RUNX3 on SAP and ALI Via JAK2/STAT3

Considering JAK2/STAT3 signaling is activated by pro-inflammatory cytokines, we hypothesized that the protective effects of RUNX3 on SAP and SAP-associated ALI might be associated with JAK2/STAT3 signaling. Therefore, involvement of RUNX3 in phosphorylation of JAK2/STAT3 was examined. As shown in Figure 5, phosphorylation levels of JAK2 and STAT3 were elevated in pancreas and lung of SAP rats compared to tissues from Sham rats, which was suppressed by RUNX3 overexpression in SAP rats (Figure 5A and B). All this evidence suggests that RUNX3 overexpression in SAP rats can contribute, in a critical way, to SAP-associated inflammation and tissue damage via regulation of JAK2/STAT3 phosphorylation.

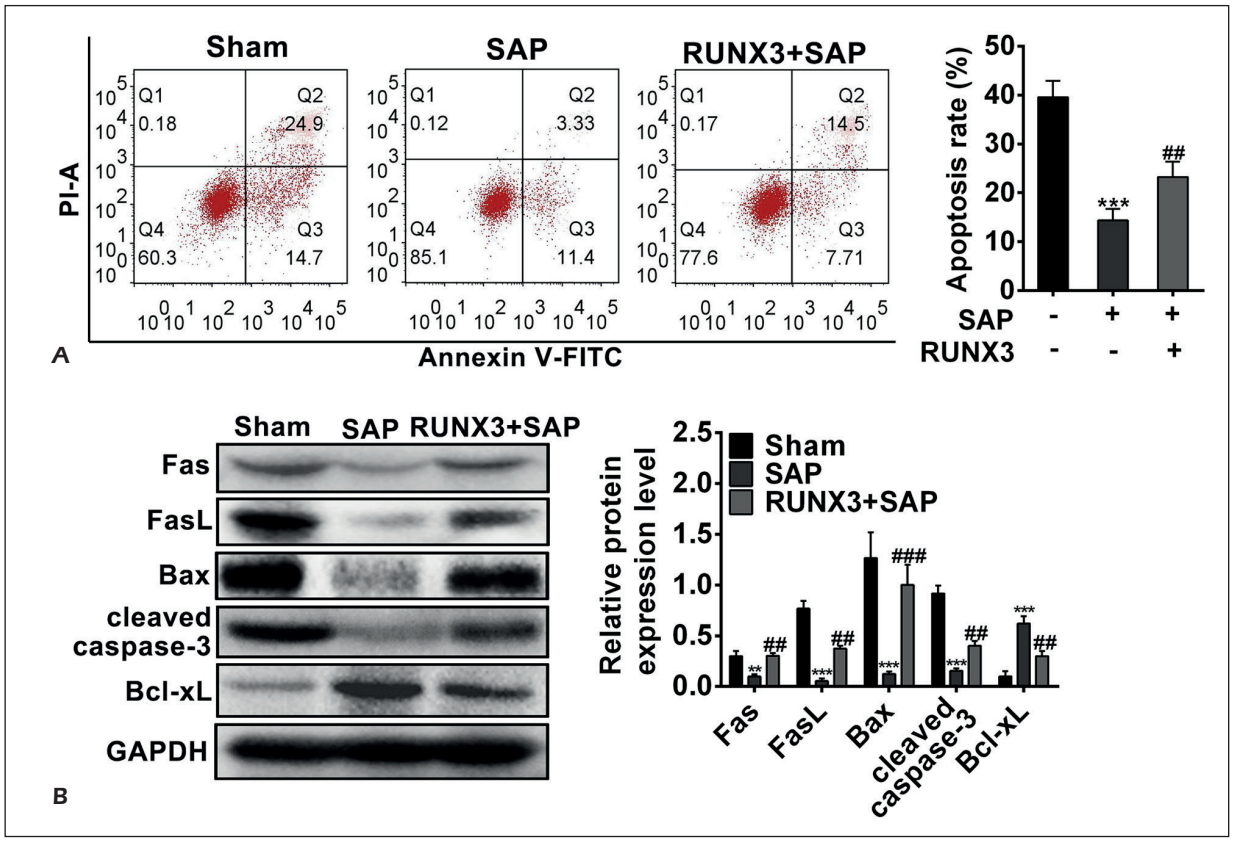

Figure 4. RUNX3 overexpression induces PMN apoptosis. PMN apoptosis was determined by FACs (**A**). Expression levels of apoptosis-associated proteins was detected by Western blotting (**B**). (Mean±S.D; n=3; SAP *vs.* sham, **p<0.01, ***p<0.001; RUNX3 overexpression *vs.* sham, $^{\#\#}p$<0.01, $^{\#\#\#}p$<0.001).

Discussion

SAP is known for its acute onset and rapid progression, leading to multiple organ damages with systemic inflammation and ultimately high mortality. Diffuse alveolar damage, type I pneumocyte necrosis and influx of inflammatory cells were initially observed in the early stages of SAP-associated ALI[25]. This is associated with inflammatory responses, giving rise to pancreatitis and subsequent distant organ dysfunction due to the recruitment of immune cells and excessive production of inflammatory mediators[26,27]. In this study, we successfully established an SAP rat model and detected RUNX3 expression in this model (Figure 1). Levels of RUNX3 were influenced by severity of SAP; SAP resulted in suppressed RUNX3 expression compared to healthy rats in a time-dependent manner (Figure 1). To our knowledge, it is the first study showing RUNX3 involved in the SAP. In comparison with untreated SAP rats, we observed RUNX3 overexpression in SAP rats significantly abrogated SAP-induced damages of pancreas and lung (Figure 2), as well as reduced cytokines production (Figure 3). Combined these data together, an emerging role of RUXN3 in the pathogenesis of SAP could be confirmed.

As a major of immune cells in the host immune response, PMN accounts for 50%-70% of leukocytes. PMN was first recruited to the area of injury or inflammation to play a critical role in the progression of inflammation, as activation and migration of neutrophils were a hallmark in the development of inflammation[28,29]. Severe tissue damages could be induced when PMN aggregation or infiltration was overwhelmed[30]. Increasing PMN apoptosis and uptake of apoptotic PMN by macrophages abrogated PMN infiltration and further inhibited inflammatory responses, and thus contributing to recovery of tissue damages[31]. Recently, studies have found PMN was central to the evolution of SAP, mediating tissue damages in pancreas as well as remote organ injuries. Patients' peripheral blood exhibited higher levels of PMN compared to those isolated from healthy individuals. Activated PMN were reported to sig-

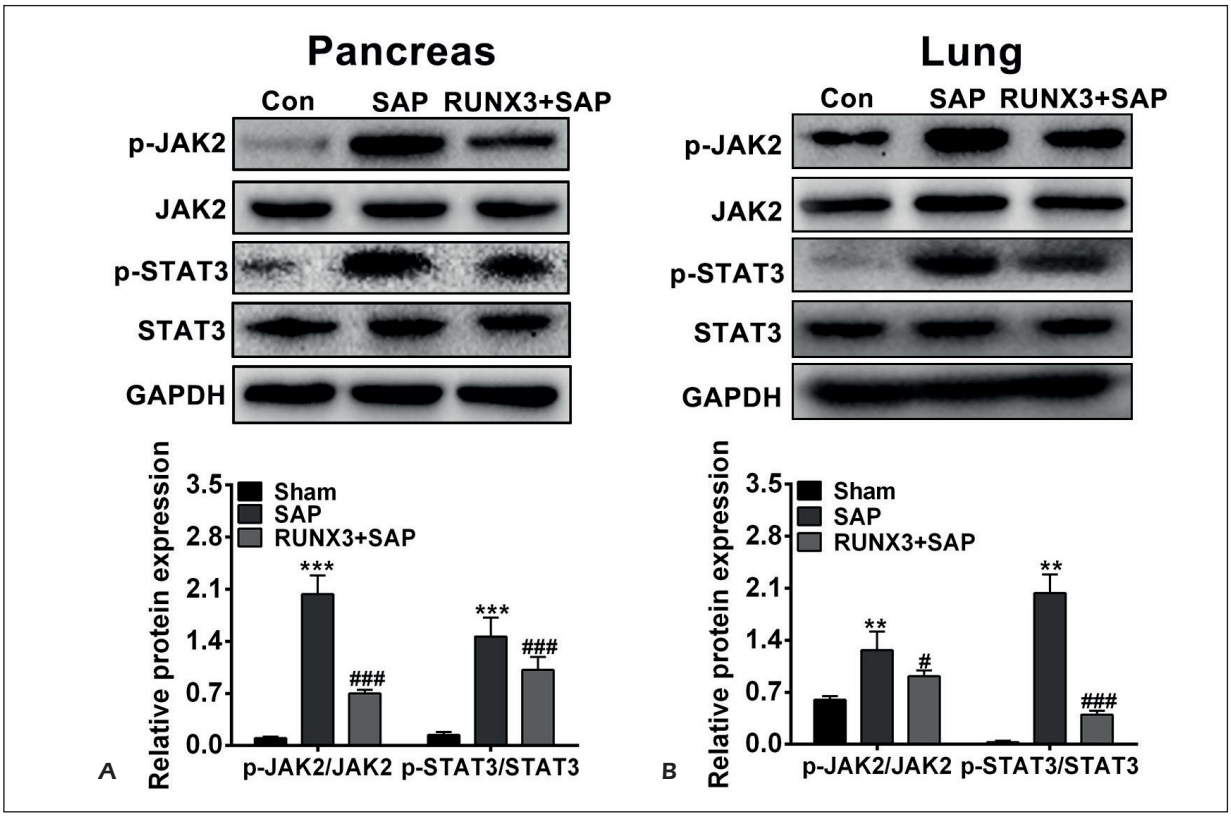

Figure 5. RUNX3 overexpression inhibits the phosphorylation of JAK2 and STAT3. The phosphorylation of JAK2 and STAT3 in pancreas (**A**) and in lung (**B**) was identified by Western blotting. (Mean±S.D; n=3; SAP *vs.* sham, **p<0.01, ***p<0.001; RUNX3 overexpression *vs.* SAP, $^{\#\#}p$<0.01, $^{\#\#\#}p$< 0.001).

nificantly extend the lifespan, which might lead to cytokines activation and delay of PMN apoptosis[32,33]. Consistent with previous studies, we observed PMN apoptosis was decreased in SAP (Figure 4A) and caspase-3 dependent apoptotic signaling was inactivated in PMN upon SAP (Figure 4B). PMN apoptosis was enhanced by RUNX3 overexpression in SAP rats (Figure 4), suggesting a possible therapeutic strategy targeting inflammation as well as tissue damages in SAP-associated ALI through extension of PMN lifespan by RUNX3 overexpression.

In addition, JAK/STAT signaling pathway is considered to be closely related to inflammation[34]. Several reports[35,36] have shown that JAK/STAT activated cytokine signaling cascade, especially JAK2 and STAT3. Previous studies[37,38] reported cytokines triggered JAK2-mediated activation of STAT1 or STAT3 and thus contributing to the development of pancreatic injuries. Inhibition of JAK/STAT signaling prevented lethal effects of excessive systemic inflammatory responses under SAP[17]. Chao et al[39] reported blockade of IL-6 inhibited activation of STAT3 in the caerulein-induced SAP-associated ALI, indicating STAT3 functioned as a regulator of SAP-associated ALI, although the detailed mechanism remained unclear. Therefore, we explored the possible modulatory mechanism targeting RUNX3-JAK2/STAT3 crosstalk. As shown in Figure 5, we found the phosphorylation statuses of JAK2 and STAT3 in pancreas and lung of SAP rats were significantly increased compared with that in Sham group, suggesting JAK2 phosphorylation would lead to phosphorylated STAT3, translocated activated STAT3 into nuclei to modulate cytokine-mediated signal transduction, which further promoted the development of SAP and SAP-associated ALI. Interestingly, phosphorylation statuses of JAK2 and STAT3 were clearly suppressed by RUNX3 overexpression in SAP rats. It is suggested another possible protective role of RUNX3 in SAP-associated ALI, that is regulation of JAK2/STAT3 phosphorylation statuses.

MicroRNAs are small non-coding nucleotides that specifically expressed in various types of cells and tissues, functioning in RNA silencing and post-transcriptional regulation of gene

expression[40-42]. Recently, microRNA acquire recognition for their importance in a variety of biological process, including cell proliferation, apoptosis, inflammation, and diseases[43-45]. Accumulating evidence suggested JAK/STAT signaling played a critical role in various biological functions of miRNAs. For instance, miR-155 regulated lymphoma cell proliferation and apoptosis by targeting JAK/STAT3 signaling[46]. MiR-210 suppressed inflammation via JAK/STAT pathway as well[47]. Importantly, bioinformatics analysis and luciferase reporter assays were strongly proved RUNX3 was a direct downstream target of miR-106b[48]. In addition, Fu et al[49] reported miR-138 regulated the balance of Th1/Th2 cells by targeting RUNX3. Our data showed RUNX3 protected against ALI via JAK2/STAT3 signaling, whether RUNX3-mediated inhibition of JAK2/STAT3 signaling was associated with microRNA remained currently unknown, which required further investigations.

Conclusions

We reported, for the first time, the protective effects of RUNX3 on SAP-associated ALI through controlling PMN apoptosis and regulating JAK2/STAT3 signaling. This finding not only improved our understanding of molecular mechanisms of SAP progression but also provided insights into future development of therapeutic strategies targeting SAP from bench to clinic.

Conflict of Interests

The Authors declare that there are no conflicts of interest.

References

1) Munhoz-Filho CH, Batigalia F, Funes HL. Clinical and therapeutic correlations in patients with slight acute pancreatitis. Arq Bras Cir Dig 2015; 28: 24-27.
2) Whitcomb DC. Genetic risk factors for pancreatic disorders. Gastroenterology 2013; 144: 1292-1302.
3) Toh SK, Phillips S, Johnson CD. A prospective audit against national standards of the presentation and management of acute pancreatitis in the South of England. Gut 2000; 46: 239-243.
4) Wang GJ, Gao CF, Wei D, Wang C, Ding SQ. Acute pancreatitis: etiology and common pathogenesis. World J Gastroenterol 2009; 15: 1427-1430.
5) Swaroop VS, Chari ST, Clain JE. Severe acute pancreatitis. JAMA 2004; 291: 2865-2868.
6) Norman J. The role of cytokines in the pathogenesis of acute pancreatitis. Am J Surg 1998; 175: 76-83.
7) Lei H, Minghao W, Xiaonan Y, Ping X, Zioi L, Qing X. Acute lung injury in patients with severe acute pancreatitis. Turk J Gastroenterol 2013; 24: 502-507.
8) Yang ZW, Meng XX, Xu P. Central role of neutrophil in the pathogenesis of severe acute pancreatitis. J Cell Mol Med 2015; 19: 2513-2520.
9) Shuai K, Liu B. Regulation of JAK-STAT signalling in the immune system. Nat Rev Immunol 2003; 3: 900-911.
10) Ihle JN, Witthuhn BA, Quelle FW, Yamamoto K, Thierfelder WE, Kreider B, Silvennoinen O. Signaling by the cytokine receptor superfamily: JAKs and STATs. Trends Biochem Sci 1994; 19: 222-227.
11) Yang XP, Irani K, Mattagajasingh S, Dipaula A, Khanday F, Ozaki M, Fox-Talbot K, Baldwin WM 3rd, Becker LC. Signal transducer and activator of transcription 3alpha and specificity protein 1 interact to upregulate intercellular adhesion molecule-1 in ischemic-reperfused myocardium and vascular endothelium. Arterioscler Thromb Vasc Biol 2005; 25: 1395-1400.
12) Wang M, Zhang W, Crisostomo P, Markel T, Meldrum KK, Fu XY, Meldrum DR. Endothelial STAT3 plays a critical role in generalized myocardial proinflammatory and proapoptotic signaling. Am J Physiol Heart Circ Physiol 2007; 293: H2101-2108.
13) Aggarwal BB, Kunnumakkara AB, Harikumar KB, Gupta SR, Tharakan ST, Koca C, Dey S, Sung B. Signal transducer and activator of transcription-3, inflammation, and cancer: how intimate is the relationship? Ann N Y Acad Sci 2009; 1171: 59-76.
14) Fridman JS, Scherle PA, Collins R, Burn TC, Li Y, Li J, Covington MB, Thomas B, Collier P, Favata MF, Wen X, Shi J, McGee R, Haley PJ, Shepard S, Rodgers JD, Yeleswaram S, Hollis G, Newton RC, Metcalf B, Friedman SM, Vaddi K. Selective inhibition of JAK1 and JAK2 is efficacious in rodent models of arthritis: preclinical characterization of INCB028050. J Immunol 2010; 184: 5298-5307.
15) Jee SH, Chu CY, Chiu HC, Huang YL, Tsai WL, Liao YH, Kuo ML. Interleukin-6 induced basic fibroblast growth factor-dependent angiogenesis in basal cell carcinoma cell line via JAK/STAT3 and PI3-kinase/Akt pathways. J Invest Dermatol 2004; 123: 1169-1175.
16) Ju KD, Lim JW, Kim KH, Kim H. Potential role of NADPH oxidase-mediated activation of Jak2/Stat3 and mitogen-activated protein kinases and expression of TGF-beta1 in the pathophysiology of acute pancreatitis. Inflamm Res 2011; 60: 791-800.
17) Yu JH, Kim KH, Kim H. Suppression of IL-1beta expression by the Jak 2 inhibitor AG490 in cerulein-stimulated pancreatic acinar cells. Biochem Pharmacol 2006; 72: 1555-1562.
18) Ito Y. Molecular basis of tissue-specific gene expression mediated by the runt domain transcription factor PEBP2/CBF. Genes Cells 1999; 4: 685-696.
19) Bangsow C, Rubins N, Glusman G, Bernstein Y, Negreanu V, Goldenberg D, Lotem J, Ben-Asher E, Lancet D, Levanon D, Groner Y. The RUNX3 gene--sequence, structure and regulated expression. Gene 2001; 279: 221-232.

20) Fainaru O, Woolf E, Lotem J, Yarmus M, Brenner O, Goldenberg D, Negreanu V, Bernstein Y, Levanon D, Jung S, Groner Y. Runx3 regulates mouse TGF-beta-mediated dendritic cell function and its absence results in airway inflammation. EMBO J 2004; 23: 969-979.
21) Brenner O, Levanon D, Negreanu V, Golubkov O, Fainaru O, Woolf E, Groner Y. Loss of Runx3 function in leukocytes is associated with spontaneously developed colitis and gastric mucosal hyperplasia. Proc Natl Acad Sci U S A 2004; 101: 16016-16021.
22) Zhou X, Liu Z, Cheng X, Zheng Y, Zeng F, He Y. Socs1 and Socs3 degrades Traf6 via polyubiquitination in LPS-induced acute necrotizing pancreatitis. Cell Death Dis 2015; 6: e2012.
23) Zhou XY, Zhou ZG, Ding JL, Wang L, Wang R, Zhou B, Gu J, Sun XF, Li Y. TRAF6 as the key adaptor of TLR4 signaling pathway is involved in acute pancreatitis. Pancreas 2010; 39: 359-366.
24) In Guide for the Care and Use of Laboratory Animals. Edited by th. Washington (DC); 2011. The National Academies Collection: Reports funded by National Institutes of Health.
25) Tomashefski JF, Jr. Pulmonary pathology of the adult respiratory distress syndrome. Clin Chest Med 1990; 11: 593-619.
26) Kempuraj D, Twait EC, Williard DE, Yuan Z, Meyerholz DK, Samuel I. The novel cytokine interleukin-33 activates acinar cell proinflammatory pathways and induces acute pancreatic inflammation in mice. PLoS One 2013; 8: e56866.
27) Geisler F, Algul H, Riemann M, Schmid RM. Questioning current concepts in acute pancreatitis: endotoxin contamination of porcine pancreatic elastase is responsible for experimental pancreatitis-associated distant organ failure. J Immunol 2005; 174: 6431-6439.
28) Noel P, Patel K, Durgampudi C, Trivedi RN, de Oliveira C, Crowell MD, Pannala R, Lee K, Brand R, Chennat J, Slivka A, Papachristou GI, Khalid A, Whitcomb DC, DeLany JP, Cline RA, Acharya C, Jaligama D, Murad FM, Yadav D, Navina S, Singh VP. Peripancreatic fat necrosis worsens acute pancreatitis independent of pancreatic necrosis via unsaturated fatty acids increased in human pancreatic necrosis collections. Gut 2016; 65: 100-111.
29) Guo ZZ, Wang P, Yi ZH, Huang ZY, Tang CW. The crosstalk between gut inflammation and gastrointestinal disorders during acute pancreatitis. Curr Pharm Des 2014; 20: 1051-1062.
30) Theilgaard-Monch K, Knudsen S, Follin P, Borregaard N. The transcriptional activation program of human neutrophils in skin lesions supports their important role in wound healing. J Immunol 2004; 172: 7684-7693.
31) Nauseef WM, Borregaard N. Neutrophils at work. Nat Immunol 2014; 15: 602-611.
32) Fournier BM, Parkos CA. The role of neutrophils during intestinal inflammation. Mucosal Immunol 2012; 5: 354-366.
33) Douda DN, Yip L, Khan MA, Grasemann H, Palaniyar N. Akt is essential to induce NADPH-dependent NETosis and to switch the neutrophil death to apoptosis. Blood 2014; 123: 597-600.
34) Yu JH, Kim H. Role of janus kinase/signal transducers and activators of transcription in the pathogenesis of pancreatitis and pancreatic cancer. Gut Liver 2012; 6: 417-422.
35) Huang C, Ma R, Sun S, Wei G, Fang Y, Liu R, Li G. JAK2-STAT3 signaling pathway mediates thrombin-induced proinflammatory actions of microglia in vitro. J Neuroimmunol 2008; 204: 118-125.
36) Agrawal S, Gollapudi S, Su H, Gupta S. Leptin activates human B cells to secrete TNF-alpha, IL-6, and IL-10 via JAK2/STAT3 and p38MAPK/ERK1/2 signaling pathway. J Clin Immunol 2011; 31: 472-478.
37) Yu JH, Kim KH, Kim H. SOCS 3 and PPAR-gamma ligands inhibit the expression of IL-6 and TGF-beta1 by regulating JAK2/STAT3 signaling in pancreas. Int J Biochem Cell Biol 2008; 40: 677-688.
38) Robinson K, Vona-Davis L, Riggs D, Jackson B, McFadden D. Peptide YY attenuates STAT1 and STAT3 activation induced by TNF-alpha in acinar cell line AR42J. J Am Coll Surg 2006; 202: 788-796.
39) Chao KC, Chao KF, Chuang CC, Liu SH. Blockade of interleukin 6 accelerates acinar cell apoptosis and attenuates experimental acute pancreatitis in vivo. Br J Surg 2006; 93: 332-338.
40) Ambros V. The functions of animal microRNAs. Nature 2004; 431: 350-355.
41) Bartel DP. MicroRNAs: genomics, biogenesis, mechanism, and function. Cell 2004; 116: 281-297.
42) Lagos-Quintana M, Rauhut R, Yalcin A, Meyer J, Lendeckel W, Tuschl T. Identification of tissue-specific microRNAs from mouse. Curr Biol 2002; 12: 735-739.
43) Cheng AM, Byrom MW, Shelton J, Ford LP. Antisense inhibition of human miRNAs and indications for an involvement of miRNA in cell growth and apoptosis. Nucleic Acids Res 2005; 33: 1290-1297.
44) Buckland J. Biomarkers: microRNAs under the spotlight in inflammatory arthritis. Nat Rev Rheumatol 2010; 6: 436.
45) Wisloff U, Najjar SM, Ellingsen O, Haram PM, Swoap S, Al-Share Q, Fernstrom M, Rezaei K, Lee SJ, Koch LG, Britton SL. Cardiovascular risk factors emerge after artificial selection for low aerobic capacity. Science 2005; 307: 418-420.
46) Li XD, Li XM, Gu JW, Sun XC. MiR-155 regulates lymphoma cell proliferation and apoptosis through targeting SOCS3/JAK-STAT3 signaling pathway. Eur Rev Med Pharmacol Sci 2017; 21: 5153-5159.
47) Dai J, Yu GY, Sun HL, Zhu GT, Han GD, Jiang HT, Tang XM. MicroRNA-210 promotes spinal cord injury recovery by inhibiting inflammation via the JAK-STAT pathway. Eur Rev Med Pharmacol Sci 2018; 22: 6609-6615.
48) Xu Y, Wang K, Gao W, Zhang C, Huang F, Wen S, Wang B. MicroRNA-106b regulates the tumor suppressor RUNX3 in laryngeal carcinoma cells. FEBS Lett 2013; 587: 3166-3174.
49) Fu D, Yu W, Li M, Wang H, Liu D, Song X, Li Z, Tian Z. MicroRNA-138 regulates the balance of Th1/Th2 via targeting RUNX3 in psoriasis. Immunol Lett 2015; 166: 55-62.